International Journal of Civil Engineering and Technology (IJCIET)
Volume 7, Issue 1, Jan-Feb 2016, pp. 113-127, Article ID: IJCIET_07_01_010
Available online at
http://www.iaeme.com/IJCIET/issues.asp?JType=IJCIET&VType=7&IType=1
Journal Impact Factor (2016): 9.7820 (Calculated by GISI) www.jifactor.com
ISSN Print: 0976-6308 and ISSN Online: 0976-6316

NONLINEAR BEHAVIOR AND FRAGILITY ASSESSMENT OF MULTI-STORY CONFINED MASONRY WALLS UNDER CYCLIC LOADS

Mohamed Said and Mosaad El-Diasity
Assistant Prof., Civil Eng. Dept., Shoubra Faculty of Eng.,
Benha University, Egypt

Osama Kamal
Professor, Shoubra Faculty of Engineering,
Benha University, Egypt

Hussein Okail
Assistant Professor, Civil Eng. Dept.,
Ain Shams University, Egypt

ABSTRACT

This paper presents numerical study analysis and the results of confined masonry walls. The studied parameters were number of bays, number of stories, and openings of walls. It was showed that the window opening could reduce the lateral capacity of the solid by ranges of 7-27% for one bay wall, 6-30% for two bay walls, and 11-26% for three bays wall. The door opening could reduce the solid wall capacity by ranges of 11-42% for one bay wall, 13-49% for two bay walls, and 23-44% for three bays wall. This paper presents the most significant contributions in the field of vulnerability assessment. It is shown that methodology is very useful for assessing the seismic vulnerability of confined masonry structures for estimating the cyclic load induced economic losses based on an engineering demand parameter closely related to structural damage.

Keywords: Confined Masonry, Seismic Behavior, Cyclic loading and Fragility

Cite this Article: Mohamed Said, Osama Kamal, Mosaad El-Diasity and Hussein Okail. Nonlinear Behavior and Fragility Assessment of Multi-Story Confined Masonry Walls under Cyclic Loads. *International Journal of Civil Engineering and Technology*, **7**(1), 2016, pp. 113-127.
http://www.iaeme.com/IJCIET/issues.asp?JType=IJCIET&VType=7&IType=1

1. INTRODUCTION

Confined masonry buildings have demonstrated satisfactory performance in past earthquakes. In general, buildings of this type had been damaged in earthquakes, however when properly designed and constructed they are able to sustain earthquake effects without collapse. Latin America is certainly a region of the world where confined masonry (CM) construction is widely used and was tested in several significant earthquakes associated with the region's high seismic risk. According to Schultz A. 1994 [1], low-rise CM buildings have performed well in past Latin American earthquakes. This applies to buildings regular in plan and elevation, which are lightly loaded and have rather large wall density.

Seismic behavior of CM wall can be explained by composite (monolithic) action of a masonry wall and adjacent RC confining elements. This composite action exists due to the toothing between the walls and the tie-columns. In absence of toothing, composite action can be achieved by means of horizontal reinforcement (dowels). A typical damage pattern demonstrated in the form of diagonal shear cracks [2]. The failure took place in the form of a signal diagonal crack which propagated through the walls and the tie-columns. This mechanism can be expected to occur in buildings with small RC tie-column sizes, where tie-column depth does not exceed 1.5 times the wall thickness.

Experimental tests and damage observations indicates that shear cracks usually initiate at opening corners and extend towards the middle of piers. Size, shape, location, and confinement detailing around openings have a great impact on the seismic performance of CM walls. This behavior is in fact highly correlated to the inclination of the diagonal struts forming either side of the openings, and the shear capacity of tie-columns (Ishibashi et al. [3]). While excessively large openings could reduce shear capacity of confined masonry walls by almost 50% (Gostic and Zarnic, [4]), their effect on seismic performance is almost negligible when size is restrained to approximately 10% of the wall gross area (Yanez, et al. [5]).

A parametric study was conducted using NLFEA to investigate the performance of confined masonry wall in seismic zones. The parameters considered were the number of bays, number of stories, and openings of walls. NLFEA investigation was carried out to establish 3D finite element models using "ANSYS 12.1" software [6]. Several earlier studies were approved to study behavior of masonry and reinforced concrete elements using ANSYS software [7- 9]. In addition, this paper is to present a numerical based methodology to develop fragility curves for confined masonry buildings. Those fragility curves can be used in combination with the hazard data of a region to perform a complete seismic risk assessment. Verification study was performed for six wall assemblies and its laboratory data results (El-Diasity M. et al., 2015[10]). A good agreement was found by comparing deformed shapes, crack patterns and capacity curves of finite element models included in this study. The referenced experimental wall assemblies were tested under a combination of a vertical load and lateral reversed cyclic loading with a displacement controlled loading protocol up to failure.

2. FINITE ELEMENT MODEL

The non-linear finite elements analysis was carried out using a computer package "ANSYS. An 8-node solid element with three translational and additional rotational degrees of freedom at each node was chosen to idealize the concrete and masonry (SOLID65) whereas a 2-node bar element was used to model the steel rebars

(LINK8). Typical modeling of the column and beam elements representing the concrete and steel rebars is indicated in Fig. 1 and Fig. 2 with the boundary conditions. The loading of the model was similar to that conducted in the experimental program, where a total vertical load of 250 kN for each story was applied uniformly on the top beam then an incremental displacement cyclic load was applied at the top of the confined column

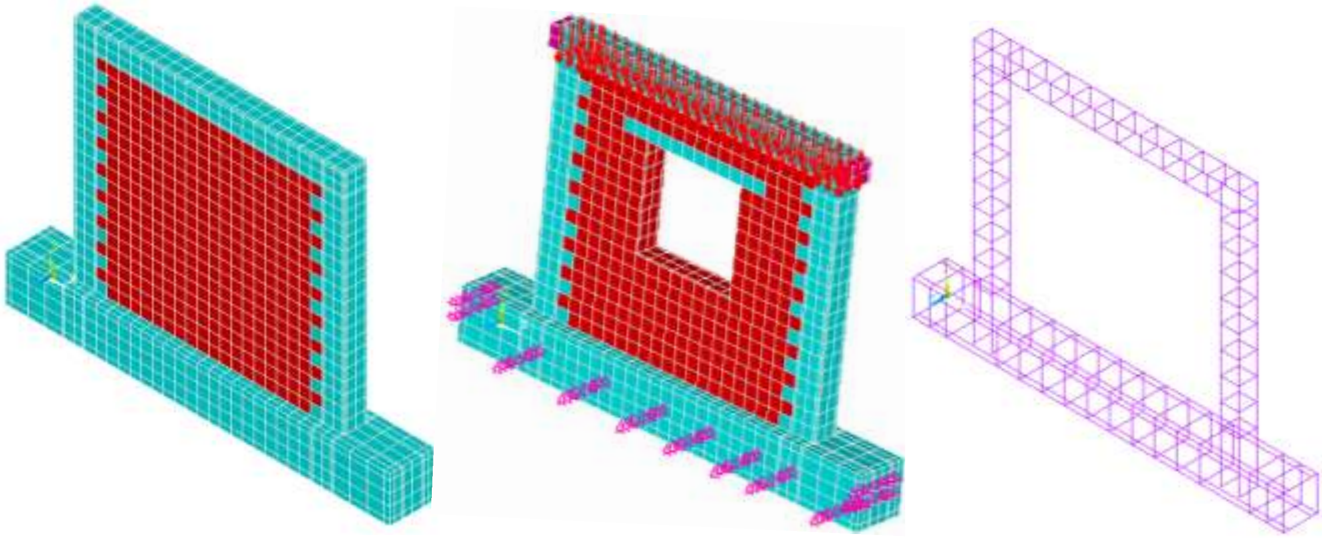

Figure 1 Finite element model characterization and meshing for one bay-one story

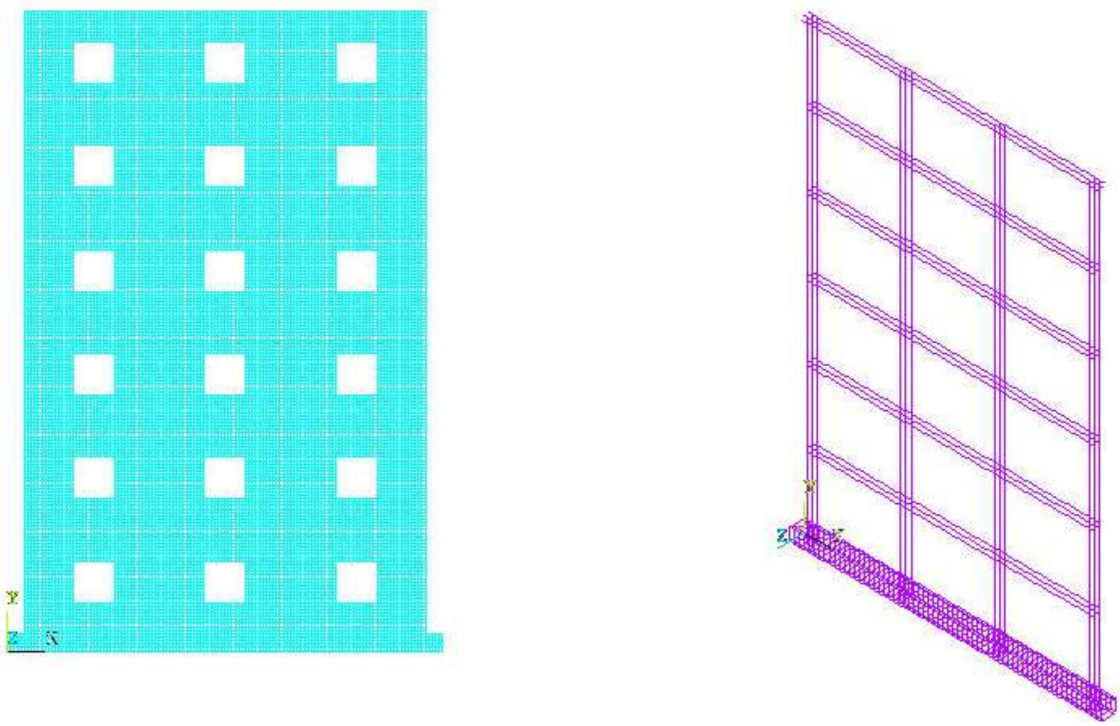

Figure 2 Finite element model characterization and meshing for three bays-six stories

3. PARAMETRIC STUDY

Three parametric studies were investigated to study the behavior of confined masonry under cyclic loads as shown in Fig. 3. Three groups of different number of stories (N) or total wall height will be studied; (two-story, four-story, and six-story) wall. Also each previous group was investigated with one-bay, two-bay, and three-bay wall. Three configurations will be studied for investigating the effect of opening on the capacity of confined masonry walls. The three configurations are solid wall, perforated wall with central window opening with size 1.2x1.2 m. The window opening represents about 12% from the total area of the wall. Finally, wall with central door had opening 1.2x2.1 m (with opening percentage 21%). The maximum lateral load capacities for all case studies were shown at Table 1.

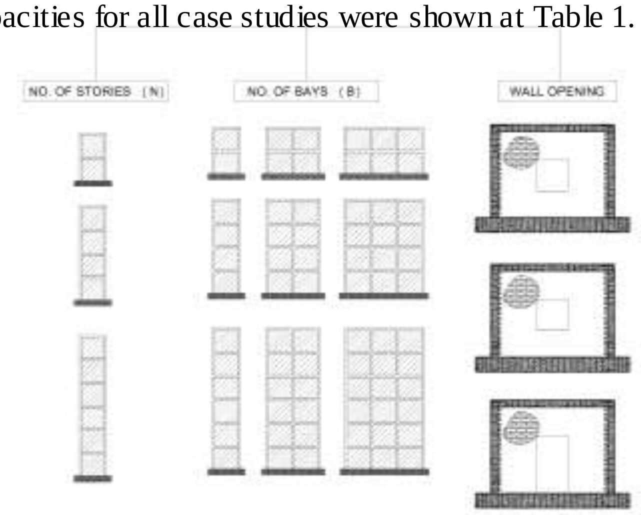

Figure 3 Numerical study of confined masonry walls

Table 1 Maximum load capacity of numerical study cases

Story	Bay	Solid Walls (KN)	Walls with window (KN)	Walls with door (KN)
2 stories	One bay	170	125	100
	Two bays	430	300	220
	Three bays	625	465	350
4 stories	One bay	100	80	76
	Two bays	240	216	163
	Three bays	380	345	248
6 stories	One bay	75	70	67
	Two bays	165	155	145
	Three bays	305	270	235

3.1 Effect of number of stories

Three groups of different number of stories (N) or total wall height will be studied; (two-story, four-story, and six-story) wall. The envelope load-drift curves for the one-bay, two-bay and three-bay walls with different number of stories were shown in Fig. 4 to Fig. 6. Obviously the lateral wall capacity is reduced as increasing of number of stories for all cases. Comparison of results evinces that the increasing of number of stories could reduce the lateral wall capacity by ranges of 51-57% for solid wall, 41-44% for window walls, and 32-34% for door walls. The upper limit in ranges was achieved at one-bay walls and the lower limit for three-bay walls. The crack patterns showed that, as the number of stories increase the failure mode controlled by flexural cracks in lower level as the slenderness of wall increase.

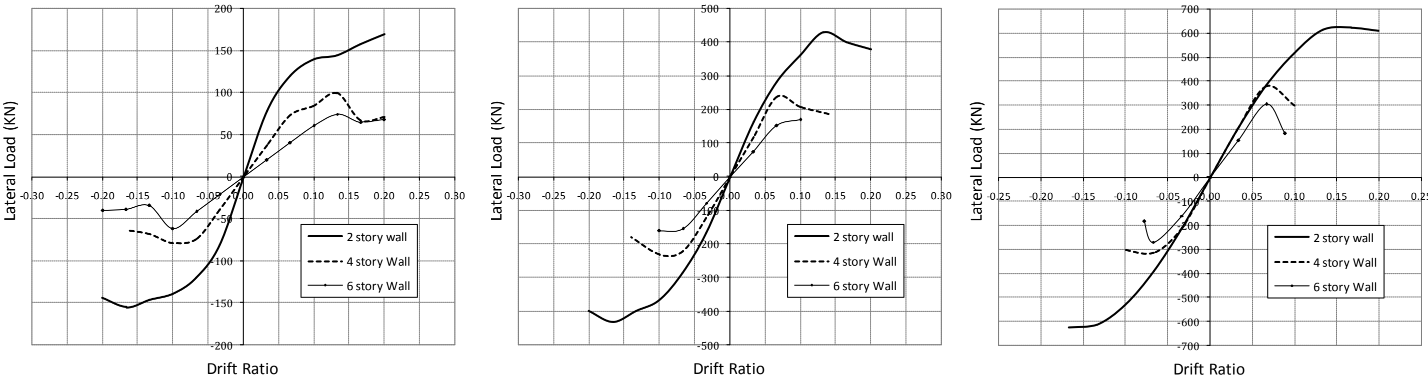

(a) one-bay solid wall (b) two-bay solid wall (c) three-bay solid wall

Figure 4 Envelope curve for lateral load-drift ratio of solid wall

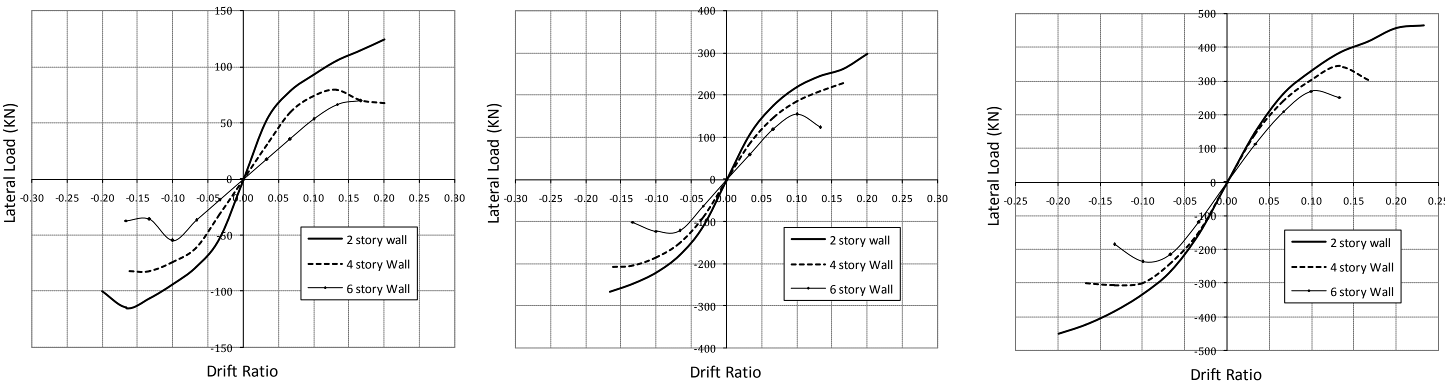

(a) one-bay window wall (b) two-bay window wall c) three-bay window wall

Figure 5 Envelope curve for lateral load-drift ratio of window wall

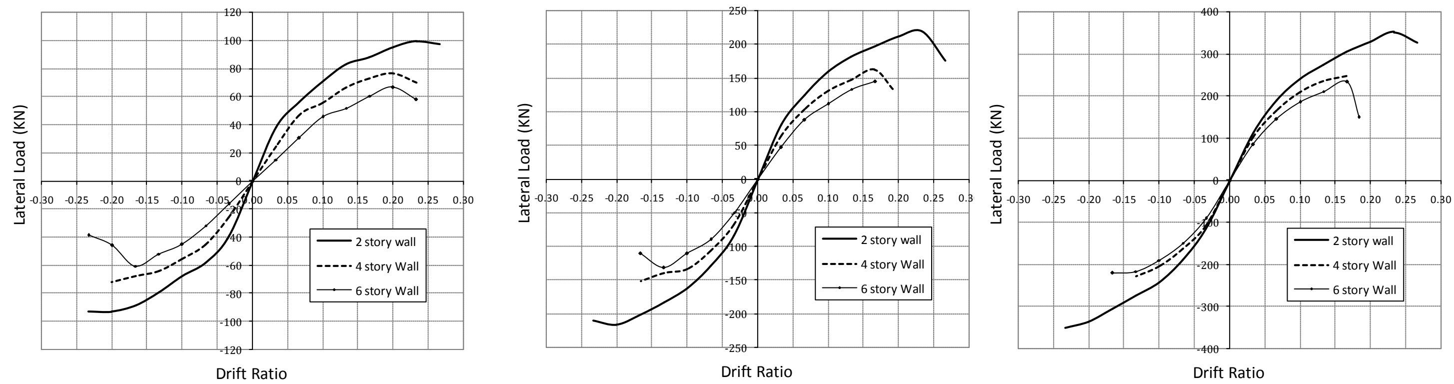

(a) one-bay door wall (b) two-bay door wall (c) three-bay door wall

Figure 6 Envelope curve for lateral load-drift ratio of door wall

3.2 Effect of number of bays

It is obvious that the wall capacity was increased as increasing of number of bays for all cases. As shown in Fig. 7 to Fig. 9, increasing of number of bays could increase the lateral capacities of walls by ranges of 268-307% for solid walls, 272-286% for window walls, and 250-253% for door walls. The upper limit in ranges was achieved at 6 story walls and the lower limit for 2 story walls. The crack patterns showed that, as the number of bays increase the failure mode controlled by diagonal shear cracks especially at lower level as the slenderness of wall decreased.

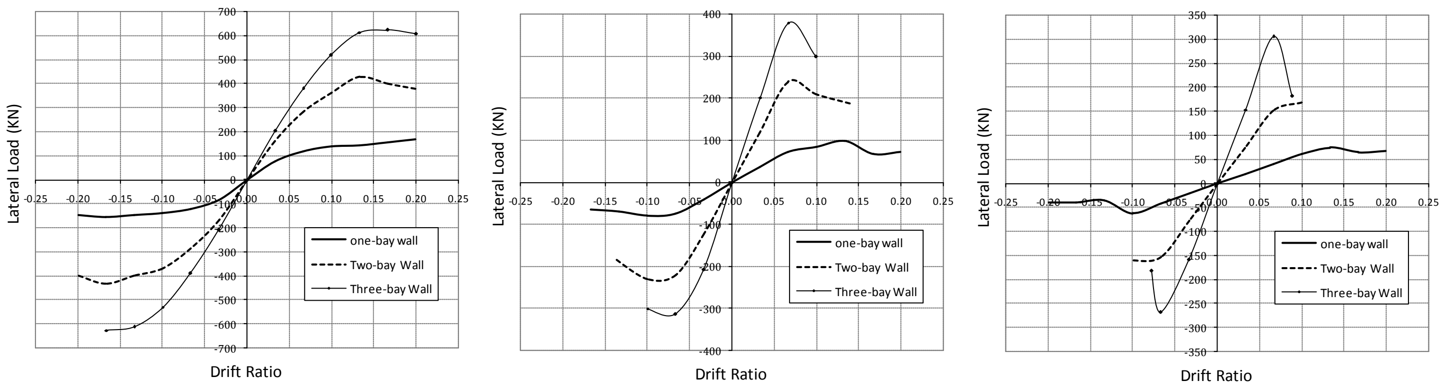

(a) 2-stories solid wall (b) 4-stories solid wall (c) 6-stories solid wall

Figure 7 Envelope curve for lateral load-drift ratio of solid wall

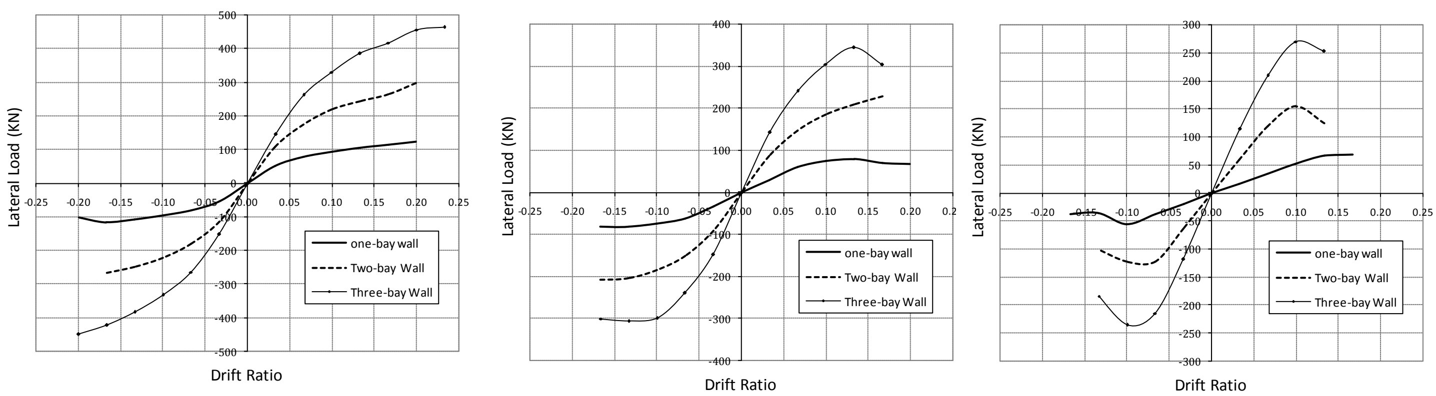

(a) 2-stories window wall (b) 4-stories window wall (c) 6-stories window wall

Figure 8 Envelope curve for lateral load-drift ratio of window wall

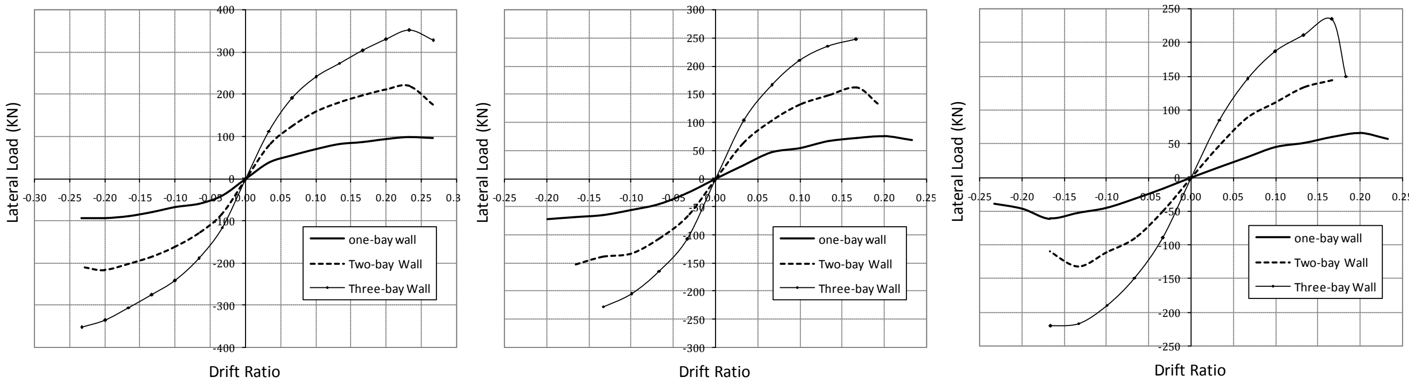

(a) 2-stories door wall (b) 4-stories door wall (c) 6-stories door wall

Figure 9 Envelope curve for lateral load-drift ratio of door wall

3.3 Effect of wall aspect ratio (height / length) (H/L) in the ultimate lateral capacity

The effect of wall aspect ratio (H/L) in accordance with the maximum lateral load of wall is shown in Fig. 10. According to the range of the parametric study, the maximum lateral loads were achieved at wall aspect ratio (H/L) equals 0.5 for solid, window, and door walls. Also the minimum lateral loads were developed at wall aspect ratio (H/L) equals 4.5 for solid, window, and door walls. As far as the height of wall is concerned, the maximum lateral load capacity of wall decreased as the slenderness of wall increased.

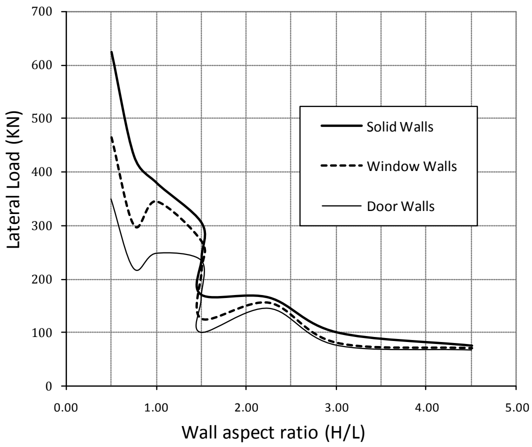

Figure 10 Effect of wall aspect ratio (H/L) in the ultimate lateral capacity

3.4 Effect of opening in walls

The analytical results indicated that the window opening could reduce the solid wall capacity by ranges of 7-27% for one bay wall, 6-30% for two bay walls, and 11-26% for three bays wall. The upper limit in ranges was achieved at 2-story walls and the lower limit for 6-story wall. As shown in Fig. 11 to Fig. 13 the door opening could reduce the solid wall capacity by ranges of 11-42% for one bay wall, 13-49% for two bay walls, and 23-44% for three bays wall. The upper limit in ranges was achieved at

2-story walls and the lower limit for 6-story wall. The envelope of lateral load-drift ratio was presented in Fig. 11 to Fig. 13.

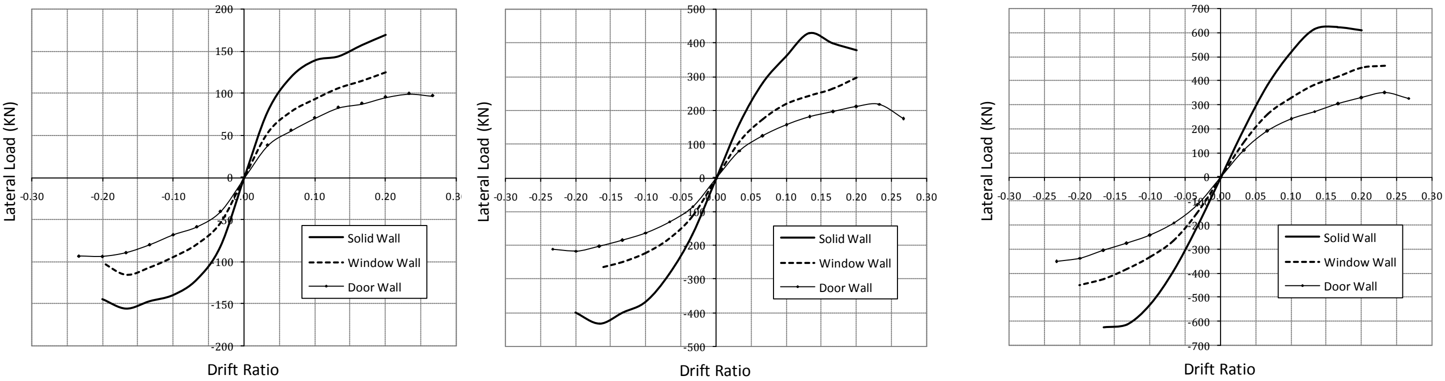

(a) one-bay wall (b) two-bay wall (c) three-bay wall

Figure 11 Envelope curve for lateral load-drift ratio of 2-stories wall

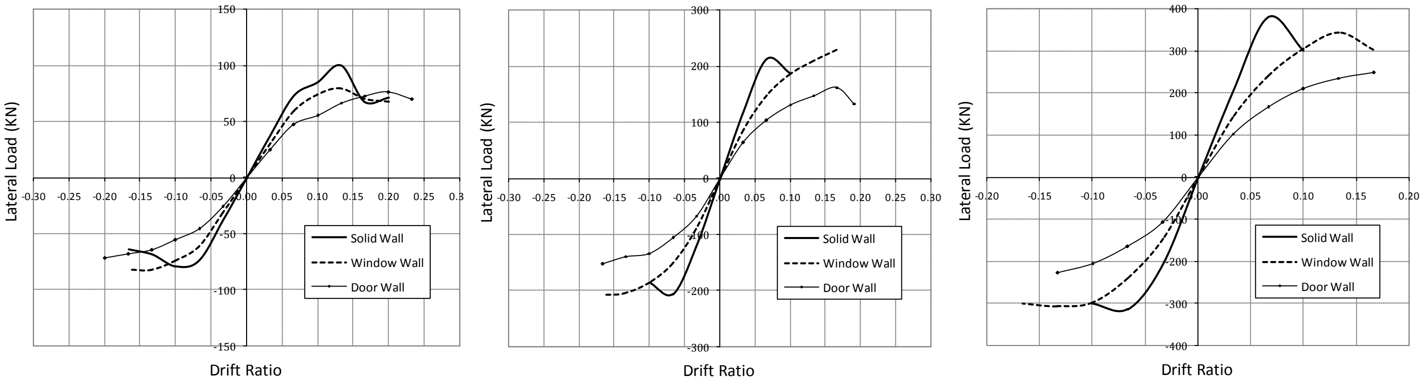

(b) one-bay wall (b) two-bay wall (c) three-bay wall

Figure 12 Envelope curve for lateral load-drift ratio of 4-stories walls

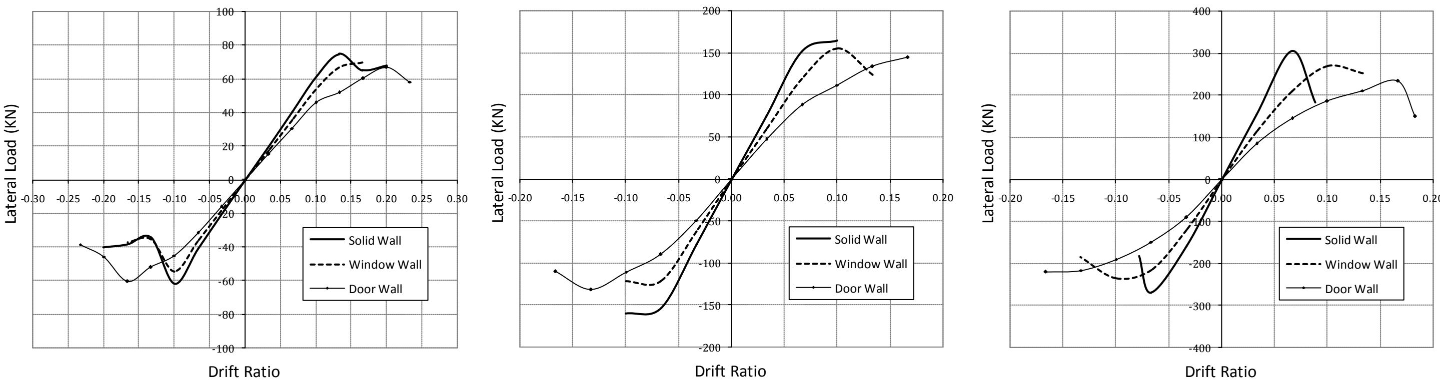

(c) one-bay wall (b) two-bay wall (c) three-bay wall

Figure 13 Envelope curve for lateral load-drift ratio of 4-stories walls

For one-bay walls the presence of window opening changing the crack behavior of wall especially diagonal shear cracks around corners of window opening that may convert the flexural mode failure of solid wall to diagonal shear failure at masonry and confined elements. The effect of door opening was clearly appeared as concentrated shear cracks around door opening and especially at the coupling beams connecting two sides of masonry piers that convert the mode of failure to be occurred according to major cracks in connecting beam above door opening. The high aspect ratio of wall controlled the flexural mode of specimen. Many diagonal shear cracks were appeared especially above door opening in 2-stories wall but less significant than 4-stories and 6-stories wall. Similar cracks observations were noticed for two-bay and three-bay specimens. Typical crack patterns for analyzed specimens were shown in Fig. 14 and Fig. 15.

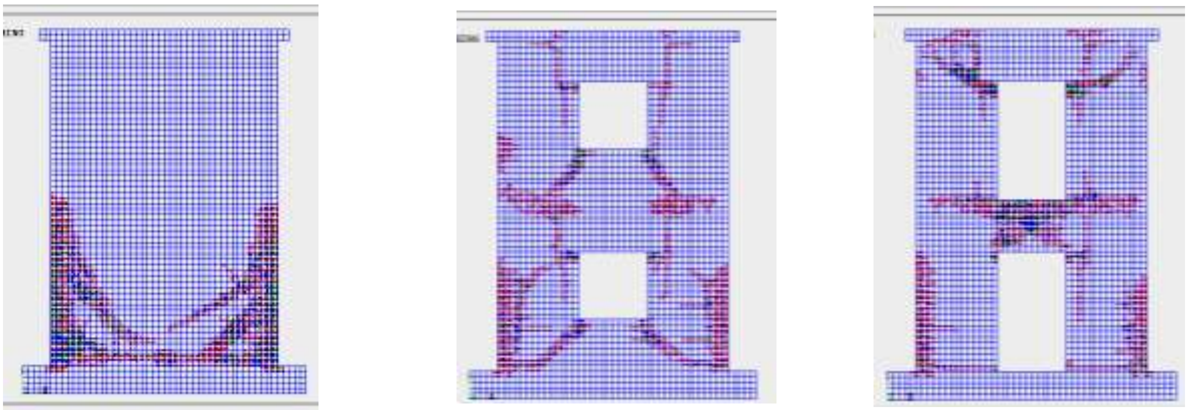

(a) solid wall (b) window wall (c) door wall

Figure 14 Crack pattern for one-bay 2-stories

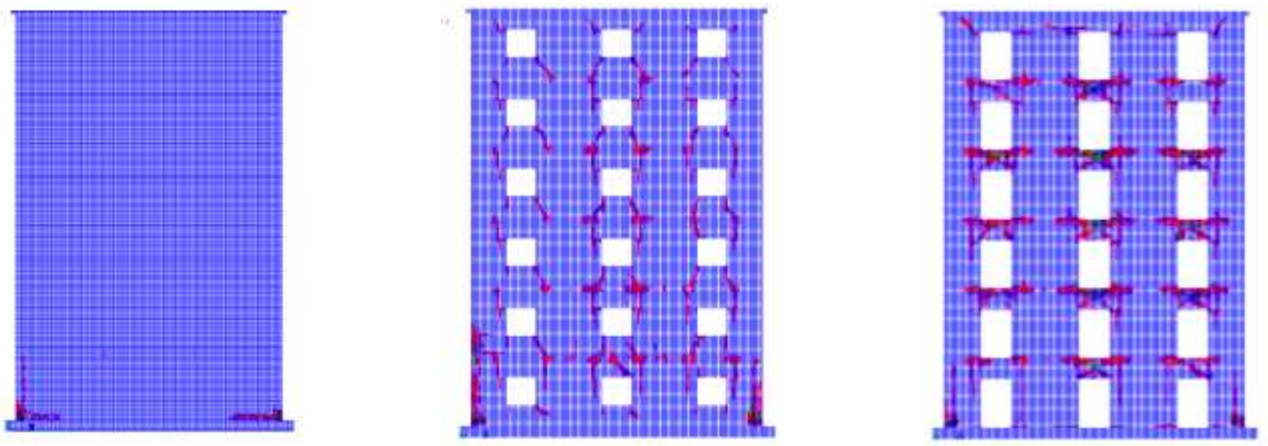

(a) solid wall (b) window wall (c) door wall

Figure 15 Crack pattern for three-bays and 6-stories

4. DAMAGE STATES OF CONFINED MASONRY WALL

Another analysis of the analytical results that clarify the seismic response of confined masonry walls is the damage states of each wall during test until failure occur. Table 2 to Table 4 summarize the damage status of walls which can be classified as slight damage (DS1) where minor cracks in masonry appear, moderate damage (DS2) where minor flexure cracks in confining elements, lintel cracks or propagation in masonry cracks happen, sever damage (DS3) where load capacity of specimen reaches maximum value or full depth diagonal cracks of masonry appear, finally collapse prevention (DS4) where shear failure in confining elements or severe base sliding/rocking take place.

Table 2 Damage states summary of solid walls

Damage state			**DS1**		**DS2**		**DS3**		**DS4**	
		Direction	**Load (KN)**	**Drift Ratio (%)**	**Load (KN)**	**Drift Ratio (%)**	**Load (KN)**	**Drift Ratio (%)**	**Load (KN)**	**Drift Ratio (%)**
2 Stories	One-bay	Push	70	0.03	80	0.035	170	0.20	170	0.20
		Pull	-70	-0.035	-75	-0.04	-160	-0.16	-148	-0.20
	Two-bays	Push	175	0.035	185	0.04	430	0.13	380	0.20
		Pull	-170	-0.042	-186	-0.045	-430	-0.17	-400	-0.20
	Three-bays	Push	290	0.045	310	0.05	625	0.15	610	0.20
		Pull	-285	-0.052	-305	-0.06	-620	-0.15	-620	-0.17
4 Stories	One-bay	Push	70	0.06	76	0.07	100	0.13	70	0.20
		Pull	-70	-0.075	-75	-0.085	-90	-0.10	-70	-0.16
	Two-bays	Push	145	0.045	195	0.05	245	0.075	190	0.14
		Pull	-150	-0.06	-190	-0.065	-240	-0.08	-180	-0.14
	Three-bays	Push	290	0.047	310	0.05	375	0.07	300	0.10
		Pull	-280	-0.055	-300	-0.06	-320	-0.08	-300	-0.10
6 Stories	One-bay	Push	60	0.10	67	0.12	70	0.14	65	0.20
		Pull	-55	-0.12	-50	-0.13	-70	-0.10	-40	-0.20
	Two-bays	Push	130	0.06	135	0.063	165	0.10	160	0.10
		Pull	-130	-0.072	-134	-0.08	-160	-0.075	-160	-0.10
	Three-bays	Push	240	0.06	246	0.065	300	0.07	180	0.09
		Pull	-238	-0.073	-250	-0.085	-250	-0.07	-180	-0.08

Table 3 Damage states summary of window walls

Damage state			DS1		DS2		DS3		DS4	
		Direction	Load (KN)	Drift Ratio (%)	Load (KN)	Drift Ratio (%)	Load (KN)	Drift Ratio (%)	Load (KN)	Drift Ratio (%)
2 Stories	One-bay	Push	50	0.02	70	0.05	125	0.20	125	0.20
		Pull	-50	-0.03	-67	-0.062	-120	-0.16	-100	-0.20
	Two-bays	Push	70	0.013	140	0.04	300	0.20	300	0.20
		Pull	-70	-0.015	-135	-0.05	-270	-0.17	-270	-0.17
	Three-bays	Push	70	0.01	190	0.03	475	0.23	475	0.23
		Pull	-70	-0.015	185	0.035	-450	-0.20	-450	-0.20
4 Stories	One-bay	Push	50	0.05	70	0.09	78	0.13	67	0.20
		Pull	-50	-0.06	-71	-0.10	-77	-0.14	-70	-0.16
	Two-bays	Push	80	0.035	150	0.065	225	0.17	225	0.17
		Pull	-75	-0.04	-145	-0.072	-210	-0.15	-200	-0.16
	Three-bays	Push	120	0.03	210	0.06	345	0.13	300	0.17
		Pull	-120	-0.035	-212	-0.07	-310	-0.11	-300	-0.17
6 Stories	One-bay	Push	50	0.08	68	0.125	70	0.17	70	0.17
		Pull	-50	-0.09	-67	-0.13	-60	-0.10	-40	-0.17
	Two-bays	Push	100	0.055	145	0.08	150	0.10	120	0.14
		Pull	-100	-0.06	-135	-0.085	-125	-0.10	-100	-0.14
	Three-bays	Push	140	0.04	185	0.06	280	0.10	270	0.14
		Pull	-140	-0.045	-180	-0.065	-250	-0.08	-180	-0.14

Table 4 Damage states summary of door walls

Damage state			DS1		DS2		DS3		DS4	
		Direction	Load (KN)	Drift Ratio (%)	Load (KN)	Drift Ratio (%)	Load (KN)	Drift Ratio (%)	Load (KN)	Drift Ratio (%)
2 Stories	One-bay	Push	30	0.022	58	0.06	100	0.23	97	0.27
		Pull	-30	-0.025	-57	-0.065	-0.95	-0.20	-92	-0.24
	Two-bays	Push	70	0.02	120	0.06	220	0.23	175	0.27
		Pull	-66	-0.023	-120	-0.065	-215	-0.20	-210	-0.24
	Three-bays	Push	110	0.028	228	0.08	350	0.23	320	0.27
		Pull	-110	-0.03	-230	-0.09	-350	-0.23	-350	-0.23
4 Stories	One-bay	Push	26	0.03	53	0.09	75	0.20	70	0.24
		Pull	-25	-0.032	-52	-0.095	-70	-0.20	-70	-0.20

	Two-bays	Push	70	0.028	100	0.06	162	0.16	140	0.19
		Pull	-70	-0.03	-100	-0.07	-155	-0.15	-145	-0.17
	Three-bays	Push	100	0.028	155	0.055	250	0.16	250	0.17
		Pull	-100	-0.03	-150	-0.06	-225	-0.14	-210	-0.14
6 Stories	One-bay	Push	20	0.056	42	0.09	67	0.20	57	0.24
		Pull	-20	-0.06	-42	-0.10	-60	-0.17	-40	-0.24
	Two-bays	Push	50	0.03	86	0.06	145	0.17	145	0.17
		Pull	-50	-0.032	-85	-0.065	-140	-0.13	-115	-0.17
	Three-bays	Push	86	0.027	135	0.052	230	0.17	200	0.18
		Pull	-85	-0.029	-132	-0.056	-220	-0.14	-210	-0.17

5. DEVELOPMENT OF FRAGILITY CURVES

A fragility curve for a component or a wall panel is meant to provide a conditional probability that a particular damage state will occur in a component for a given demand value. The top drift ratio (Δ_i) of each wall is selected as the demand parameter and also the base overturning moment per unit length (M_i), and the occurrence of each damage state is assumed to be sequential in nature. Fragility functions are used to evaluate the uncertainty associated with specific materials and member configurations in their response of seismic demands.

The ATC-58-1 (ATC 2011 [11]) recommends the use of a cumulative probability function based on a log-normal probability distribution for the generation of fragility functions. The log-normal probability distribution function is shown in Equation 1 and requires determination of the median value (drift ratio or moment at base per unit length) for each damage state (x_m) as well as the logarithmic standard deviation or dispersion (βi) as determined by Equation 2 and 3, respectively. [12-13]

$$x_m = \exp\left(\frac{1}{M}\sum_{i=1}^{M} \ln r_i\right) \qquad \text{(Eq. 1)}$$

$$\beta = \sqrt{\frac{1}{M-1}\sum_{i=1}^{M} (\ln(r_i/x_m))^2} \qquad \text{(Eq. 2)}$$

$$F_{dm}(edp) = \Phi\left(\frac{\ln(edp/x_m)}{\beta}\right) \qquad \text{(Eq. 3)}$$

Where the median value for damage states (x_m) and the logarithmic standard deviation (β_i) is each a function of the number of data points (i.e., wall specimens) and the drift ratio or moment per unit length (r_i) at the specific damage state for each wall. The log-normal probability distribution (F) for any given level of top drift ratio or moment at base per unit length is defined as the standard normal (Gaussian) cumulative distribution (Φ) with the median value and dispersion for the given damage state. Based on the output of the analytical results the drift based fragility and base moment based fragility are shown in Fig. 16 and Fig. 17.

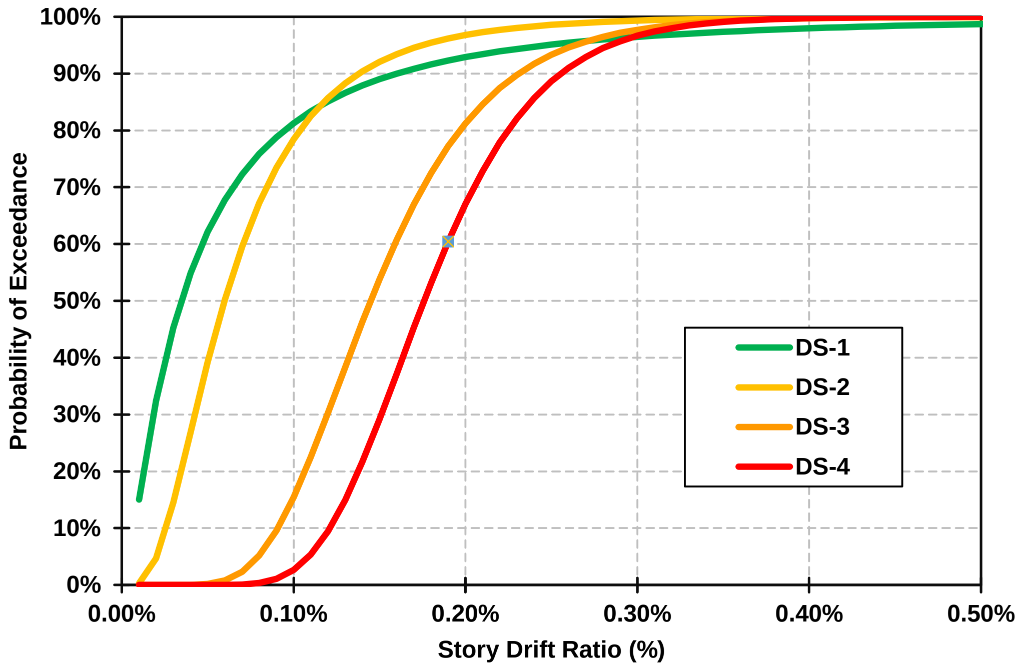

Figure 16 Drift based fragility curves for walls

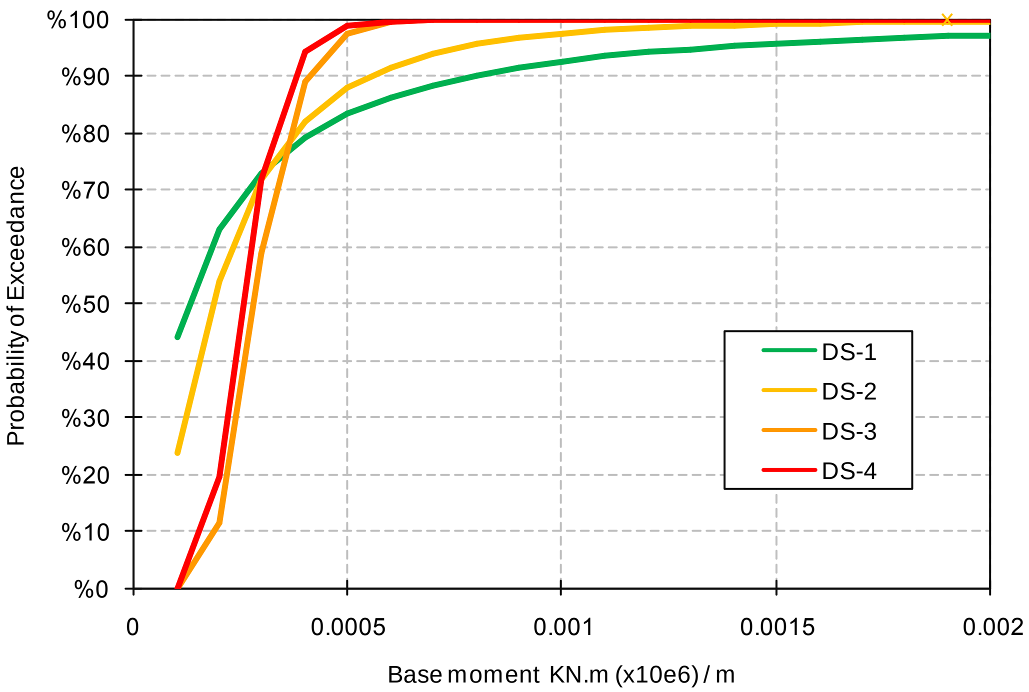

Figure 17 Base moment based fragility curves for walls

6. CONCLUSIONS

Based on this analytical investigation, the following conclusions can be drawn:

1. The lateral capacity of wall is reduced as increasing of opening size for all cases. The window opening could reduce the solid wall capacity by ranges of 7-27% for one bay wall, 6-30% for two bay walls, and 11-26% for three bays wall.
2. The door opening could reduce the solid wall ultimate lateral capacity by ranges of 11-42% for one bay wall, 13-49% for two bay walls, and 23-44% for three bays wall.
3. The flexural mode of failure occurred in solid wall may be changed to diagonal shear failure due to presence of window for 2 stories wall.
4. The effect of door opening was clearly appeared as concentrated shear cracks around door opening and especially at the coupling beams connecting two sides of masonry piers that convert the mode of failure to be occurred according to major cracks in connecting beam above door opening for 2 stories wall.
5. The presence of window opening for 4 and 6 stories walls has slightly lower effect comparing to 2 stories walls as the slenderness of wall tend to control the mode of failure to be flexural cracks at tie-columns of first story.
6. The numerical study indicated that the increasing of number of stories could reduce the wall capacity by ranges of 51-57% for solid wall, 41-44% for window walls, and 32-34% for door walls.
7. As the number of stories increased the probability of being failure mode controlled by flexural cracks in lower level as the slenderness of wall increased.
8. The mode of failure depends on the number of bay. As the number of bays increase the failure mode controlled by diagonal shear cracks especially at lower level as the slenderness of wall decreased.

7. REFERENCES

[1] Schultz, A. E. (1994), "Performance of Masonry Structures during Extreme Lateral Loading Events. Masonry in the Americas," ACI Publication SP-147, pp.21-55, American Concrete Institute, Detroit.

[2] Pérez-Gavilán, J.J, Flores, L.E. and Cruz, O. (2009), "Testing of masonry walls with different lengths: kinematics and lateral stiffness," XVII National Conference on Earthquake Engineering, Puebla, Mexico.

[3] Ishibashi, K., Meli, R., Alcocer, S.M., Leon, F., and Sanchez, T.A., (1992), "Experimental study on earthquake-resistant design of confined masonry structure," Proceedings of the tenth World conference on earthquake engineering, Madrid, Spain, pp. 3469-3474.

[4] Gostic, S. and Zarnic, R. (1999) "Cyclic lateral response of masonry infilled RC frames and confined masonry walls," Proceedings of the 8th North American Masonry Conference, Austin, June, pp. 477-488.

[5] Yanez,F., Astroza, M., Holmberg, A., and Ogaz, O., (2004), "Behavior of confined masonry shear walls with large openings," 13th world conference on earthquake engineering, Vancouver, B.C., Canada, No.343.

[6] ANSYS®, (2009), "Engineering Analysis System User's Manual, Vol. 1 & 2, and Theoretical Manual," Revision 12.1, Swanson Analysis System Inc., Houston, Pennsylvania.

[7] Hashem, Y.M., Adam, M. A., Mahmoud, A. A., and Shanour A. S., (2010), "Behavior of reinforced concrete infilled frames under cyclic loading," Ain Shams Journal of Civil Engineering, Vol. 2. September, pp. 169-182.

[8] Said, M., Adam, M. A., Mahmoud, A. A., and Shanour A. S., (2016), "Experimental and analytical shear evaluation of concrete beams reinforced with glass fiber reinforced polymers bars," Construction and Build. Material, V. 102. pp. 574-591.

[9] Maher A. Adam, Mohamed Said, Ahmed A. Mahmoud, Ali S. Shanour, (2015), "Analytical and experimental flexural behavior of concrete beams reinforced with glass fiber reinforced polymers bars," Construction and Build. Matererial, V. 84, June, pp. 354-366.

[10] El-Diasity, M., Okail H., Kamal, O. A., Said, M., (2015) "Structural performance of confined masonry walls retrofitted using ferrocement and GFRP under in-plane cyclic loading," Journal of Engineering Structures, Volume 94, July, pp. 54 - 69.

[11] ATC-58-1, (2011), "seismic performance assessment of building," Volume 1, prepared by ATC for FEMA.

[12] S Bhargavi and R Pradeep Kumar. Comparison between the Effect of Lintel and Lintel Band on the Global Performance of Load Bearing Walls and Masonry Infilled RC Frames. *International Journal of Civil Engineering and Technology*, **6**(2), 2015, pp. 68-78.

[13] Ali S. Shanour, Ahmed A. Mahmoud, Maher A. Adam and Mohamed Said. Experimental Investigation of Concrete Beams Reinforced with GFRP Bars. *International Journal of Civil Engineering and Technology*, **5**(11), 2014, pp. 154-164.